View metadata, citation and similar papers at core.ac.uk

brought to you by CORE

provided by Research Online

University of Wollongong

Research Online

Faculty of Engineering and Information Sciences - Papers: Part B

Faculty of Engineering and Information Sciences

2016

Biofouling Mitigation in Forward Osmosis Using Graphene Oxide Functionalized Thin-Film Composite Membranes

Francois Perreault
Yale University

Humberto Jaramillo
Yale University

Ming Xie
University of Wollongong, mx504@uowmail.edu.au

Mercy Ude
Yale University

Long D. Nghiem
University of Wollongong, longn@uow.edu.au

See next page for additional authors

Follow this and additional works at: https://ro.uow.edu.au/eispapers1

Part of the Engineering Commons, and the Science and Technology Studies Commons

Recommended Citation

Perreault, Francois; Jaramillo, Humberto; Xie, Ming; Ude, Mercy; Nghiem, Long D.; and Elimelech, Menachem, "Biofouling Mitigation in Forward Osmosis Using Graphene Oxide Functionalized Thin-Film Composite Membranes" (2016). *Faculty of Engineering and Information Sciences - Papers: Part B*. 247.
https://ro.uow.edu.au/eispapers1/247

Research Online is the open access institutional repository for the University of Wollongong. For further information contact the UOW Library: research-pubs@uow.edu.au

Biofouling Mitigation in Forward Osmosis Using Graphene Oxide Functionalized Thin-Film Composite Membranes

Abstract

Forward osmosis (FO) is an emerging membrane process with potential applications in the treatment of highly fouling feedwaters. However, biofouling, the adhesion of microorganisms to the membrane and the subsequent formation of biofilms, remains a major limitation since antifouling membrane modifications offer limited protection against biofouling. In this study, we evaluated the use of graphene oxide (GO) for biofouling mitigation in FO. GO functionalization of thin-film composite membranes (GO-TFC) increased the surface hydrophilicity and imparted antimicrobial activity to the membrane without altering its transport properties. After 1 h of contact time, deposition and viability of Pseudomonas aeruginosa cells on GO-TFC were reduced by 36% and 30%, respectively, compared to pristine membranes. When GO-TFC membranes were tested for treatment of an artificial secondary wastewater supplemented with P. aeruginosa, membrane biofouling was reduced by 50% after 24 h of operation. This biofouling resistance is attributed to the reduced accumulation of microbial biomass on GO-TFC compared to pristine membranes. In addition, confocal microscopy demonstrated that cells deposited on the membrane surface are inactivated, resulting in a layer of dead cells on GO-TFC that limit biofilm formation. These findings highlight the potential of GO to be used for biofouling mitigation in FO.

Disciplines

Engineering | Science and Technology Studies

Publication Details

Perreault, F., Jaramillo, H., Xie, M., Ude, M., Nghiem, L. D. & Elimelech, M. (2016). Biofouling Mitigation in Forward Osmosis Using Graphene Oxide Functionalized Thin-Film Composite Membranes. Environmental Science and Technology (Washington), 50 (11), 5840-5848.

Authors

Francois Perreault, Humberto Jaramillo, Ming Xie, Mercy Ude, Long D. Nghiem, and Menachem Elimelech

This journal article is available at Research Online: https://ro.uow.edu.au/eispapers1/247

Biofouling Mitigation in Forward Osmosis using Graphene Oxide Functionalized Thin-Film Composite Membranes

Environmental Science & Technology

Revised: April 2016

François Perreault[1,2*], Humberto Jaramillo[1], Ming Xie[1,3], Mercy Ude[1], Long D. Nghiem[4], and Menachem Elimelech[1]

[1]*Department of Chemical and Environmental Engineering, Yale University, New Haven, Connecticut 06520-8286*

[2] *School of Sustainable Engineering and the Built Environment, Arizona State University, Tempe, AZ, 85287-3005.*

[3] *Institute for Sustainability and Innovation, College of Engineering and Science, Victoria University, PO Box 14428, Melbourne, Victoria 8001, Australia*

[4] *Strategic Water Infrastructure Laboratory, School of Civil Mining Environmental Engineering, University of Wollongong, Wollongong, NSW2522, Australia*

* Corresponding author: Email: francois.perreault@asu.edu; Phone : 480-965-4028; Fax : 480-965-0557.

TOC GRAPHICS

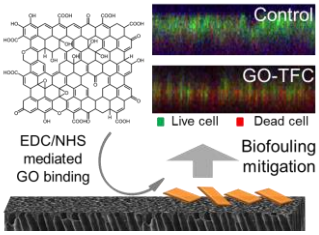

ABSTRACT

Forward osmosis (FO) is an emerging membrane process with potential applications in the treatment of highly fouling feedwaters. However, biofouling, the adhesion of microorganisms to the membrane and the subsequent formation of biofilms, remains a major limitation since antifouling membrane modifications offer limited protection against biofouling. In this study, we evaluated the use of graphene oxide (GO) for biofouling mitigation in FO. GO functionalization of thin-film composite membranes (GO-TFC) increased the surface hydrophilicity and imparted antimicrobial activity to the membrane without scarifying its transport properties. After 1 h of contact time, deposition and viability of *Pseudomonas aeruginosa* cells on GO-TFC were reduced by 36% and 30%, respectively, compared to pristine membranes. When GO-TFC membranes were tested for treatment of an artificial secondary wastewater supplemented with *P. aeruginosa*, membrane biofouling was reduced by 50% after 24 hours of operation. This biofouling resistance is attributed to the reduced accumulation of microbial biomass on GO-TFC compared to pristine membranes. In addition, confocal microscopy demonstrated that cells deposited on the membrane surface are inactivated, resulting in a layer of dead cells on GO-TFC that limit biofilm formation. These findings highlight the potential of GO to be used for biofouling mitigation in FO membrane design.

INTRODUCTION

With a growing world population, global climate change, and intensification of human activities, water availability is becoming one of the most important environmental challenges facing humanity.[1] Membrane-based technologies for water treatment, water reclamation, and desalination are some of the most effective strategies to address global water quality and scarcity issues.[1–3] However, membranes are prone to fouling, that is, the accumulation of organic, inorganic, or biological foulants on the membrane, which decrease permeate flux, membrane selectivity, and useful lifetime.[1] The design of effective fouling control strategies is therefore one of the main technical challenges in membrane-based water treatment.

Forward osmosis (FO) is an emerging membrane process that uses the osmotic difference between a concentrated draw solution and a dilute feed solution to induce spontaneous solvent permeation through a semipermeable membrane.[4] This osmotic driving force results in a foulant layer that is less compact and more easily cleanable than in pressure-driven processes such as reverse osmosis (RO).[5,6] As a result, FO has emerged as a practical approach to treat waters with high fouling potential like wastewater or activated sludge.[4,7,8] However, fouling is still detrimental to FO operations due to cake-enhanced concentration polarization, which decreases the osmotic driving force for permeation and demands frequent system interruptions for membrane cleaning. .[4,7] Therefore, improving the resistance of membranes to fouling can contribute to the successful implementation of FO technologies.

FO membrane fouling propensity is associated with the membrane surface roughness, relative hydrophobicity, and its high density of carboxyl groups.[9,10] These factors are typically found in the polyamide thin-film composite (TFC) membranes used in FO. To avoid excessive fouling, modified TFC membranes have been developed to decrease foulant adsorption.[10] Common antifouling modifications include polymer brushes, zwitterions, and superhydrophilic nanomaterials.[10–13] Such modifications were shown to improve the membrane resistance to fouling caused by organic molecules like proteins, polysaccharides, or natural organic matter.[11–13]

However, fouling in complex waters is likely to involve both organic and biological foulants. In FO-based treatment of secondary wastewater, fouling was found to be dominated by biopolymers, proteins, and microorganisms.[14] Biological fouling, or biofouling, involves the

adsorption of microorganisms to the membrane and their development into microbial communities enclosed in extracellular polymeric substances (EPS).[15] The contribution of biofouling makes fouling mitigation more challenging since membrane modifications aiming to reduce foulant adsorption often have a limited effect on biofilm formation.[16,17]

To specifically target biofouling, antimicrobial properties have been imparted to membranes.[18–20] Antimicrobial membranesinactivate bacterial cells at contact, reducing the initial rate of biofilm formation.[20] However, their long-term efficiency is limited by the eventual depletion of biocide or the accumulation of dead cells on the surface, which will shield the antimicrobial material. Recent efforts have thus been made to design membranes with both antimicrobial and antifouling properties, where membranes are modified in multiple steps with sequential grafting of polymer brushes or zwitterions, for antifouling properties, and nanoparticles or polycations, for antimicrobial activity.[21–23] While these modifications represent more complex membrane functionalization, the combination of antifouling and antimicrobial properties was highlighted as the most effective approach to mitigate membrane biofouling.[20]

Graphene oxide (GO) is a carbon-based nanomaterial composed of a single layer of sp^2-bonded carbon decorated with a high density of oxygen functional groups.[24] Due to its high surface area and colloidal stability in aqueous conditions, GO is extensively investigated as a platform material for novel membrane designs.[25,26] Notably, its incorporation into membranes was found to improve their resistance to fouling by reducing both surface roughness and hydrophobicity.[27,28] GO also possesses bactericidal properties and can induce a disruption of the cell membrane when bacteria come into contact with GO.[26,29–31] Therefore, GO may be an excellent material for the development of biofilm-resistant membranes as it can impart both antimicrobial and antifouling properties to a surface. Membrane surface functionalization with GO was previously shown to impart antimicrobial properties to its active layer;[30,32] however, its biofouling mitigation potential remains to be demonstrated in membrane operations.

In this paper, we evaluated the use of GO for biofouling mitigation in FO. GO-functionalized membranes were exposed to an artificial secondary wastewater feed, to which the biofilm-forming bacterium *Pseudomonas aeruginosa* was added, and tested in a bench-scale cross-flow FO unit. We demonstrated that when membranes are functionalized with GO (GO-TFC), water flux decline due to biofouling is reduced. Analysis of the structure and composition

of the biofilm formed on the membrane, in conjunction with a characterization of the change in surface properties imparted by GO, provided insights on the mechanisms involved in biofouling mitigation by GO. These findings highlight the potential of GO to be utilized as a biofouling control material in FO membrane design.

MATERIALS AND METHODS

Graphene Oxide Synthesis and Characterization. GO was produced by chemical oxidation of graphite by $KMnO_4$ in a mixture of H_2SO_4 and H_3PO_4, as previously described.[33] Spectroscopic characterization was realized on dry GO powders. Raman spectroscopy was performed on a Horiba Jobin Yvon HR-800 spectrometer with a 532 nm excitation. Fourier-Transformed Infrared (FTIR) spectra were collected using a Thermo Nicolet 6700 spectrometer. X-ray photoelectron spectroscopy (XPS) was performed on a ThermoScientific ESCALAB 250 with a monochromatized AI X-ray source. For microscopy analysis, GO sheets were drop-casted on a silicon wafer. Atomic Force Microscopy analysis was performed in tapping mode with a Bruker Multimode AFM (Digital Instruments, Plainview, NY) equipped with a Tap300Al-G cantilever (BudgetSensors, Sofia, Bulgaria). SEM analyses were done on a Hitachi SU-70 microscope (Hitachi High Technologies America, Inc., Clarksburg, MD). The antimicrobial activity of GO was verified by measuring the cell viability of *P. aeruginosa* cells deposited on a pure GO layer. Cell viability was measured after 1 h by staining the cells with SYTO 9 and propidium iodide (PI) and quantifying live and dead cells with an Axiovert 200M epifluorescence microscope (Carl Zeiss Inc., Thornwood, NY). Further information on GO synthesis and characterization is given in the Supporting Information (SI).

Membrane Functionalization. GO was covalently bound to FO membranes by a previously described amide coupling reaction.[32] Briefly, the carboxyl groups on the membrane polyamide layer are converted to amine-reactive esters by reaction with 4mM N-(3-dimethylaminopropyl)-N'-ethylcarbodiimide hydrochloride (EDC) and 10 mM N-hydroxysuccinimide (NHS) for 1 h. The amine-reactive esters are then used to attach ethylenediamine to the membrane. Finally, GO (10 mg) is reacted with 2 mM EDC and 5 mM NHS for 15 min, to activate its carboxyl groups, and placed in contact with the ethylenediamine-rich membrane for amide coupling. The detailed functionalization protocol is provided in the SI.

Membrane Characterization. Raman spectra were collected on a Horiba Jobin Yvon HR-800 spectrometer using a 532 nm laser excitation. For SEM imaging, samples were sputter-coated with chromium and imaged with a Hitachi SU-70 microscope. Membrane hydrophilicity was evaluated by the sessile drop method using a Theta Lite Optical Tensiometer TL100 (Attension, Espoo, Finland), using a drop volume of 5 µL. Surface roughness was measured in tapping mode with a Dimension Icon AFM equipped with a SNL-10 SiN cantilever (Bruker, Santa Barbara, CA). The membrane water permeability, *A*, salt permeability, *B*, and structural parameter, *S*, were determined according to a method previously described.[34] Draw solution concentrations of approximately 0.2, 0.4, 0.7, and 1.2 M NaCl, and DI as feed solution, were used for the different characterization steps.

Bacterial Adhesion and Viability. Membrane coupons of 3.5 cm^2 were placed in plastic holders leaving only the active layer exposed. A 3 mL suspension volume of *P. aeruginosa* (~10^8 CFU mL^{-1}) was contacted with the surface for 1 h at room temperature. The membranes were washed to remove non-attached cells and cell viability was determined by staining the cells with 3.34 µM SYTO 9 and 20 µM PI. The membranes were rinsed twice before mounting on a microscopic slide. Ten pictures per replicate were taken with an Axiovert 200M epifluorescence microscope (Carl Zeiss Inc., Thornwood, NY) and analyzed with Image J (National Institutes of Health, MD).

AFM Adhesion Force Measurements. Adhesion forces between the membrane and a 4 µm carboxylated latex particle (Life Technologies, Eugene, OR) were measured on a Dimension Icon AFM (Bruker, Santa Barbara, CA). Particle-functionalized AFM probes were prepared according to a procedure previously described.[35] Force measurements were collected in synthetic wastewater media using a trigger force of 1 nN, a ramp size of 1 µm, and a ramp rate of 0.5 Hz. More details on AFM measurements are given in the SI.

Membrane Biofouling Experiments. Biofouling experiments were carried out in a closed-loop, bench-scale FO unit. The active membrane area was 20.0 cm^2. An artificial secondary wastewater medium (ionic strength of 16 mM, pH of 7.6) was used as a feed solution (detailed in Table S1).[36] The draw solution was prepared using NaCl and the concentration adjusted to achieve an initial water flux of 20 ± 1 L m^{-2} h^{-1} (~ 1 M NaCl draw). For each membrane, a baseline run was conducted without bacteria to account for the dilution of the draw

solution during experiments. The permeate flux was stabilized at 20 ± 1 L m^{-2} h^{-1} before addition of *P. aeruginosa* to an initial concentration of ~6.0 × 10^7 CFU L^{-1}. The FO system was operated for 24 hours at a flow rate of 8.5 cm s^{-1}. The permeate flux was continuously monitored and the temperature maintained at 25 ± 1 ^{o}C. At the end of the biofouling experiment, membrane coupons were cut for biofilm characterization. Biofouling experimental procedures are further detailed in the SI.

Biofilm Characterization. Membrane coupons (1 cm^2) were cut from the center of the biofouled membrane, stained with SYTO 9, PI, and concavalin A (Con A), and mounted in a custom-made chamber for confocal laser scanning microscopy (CLSM).[37] CLSM images were captured using a Zeiss LSM 510 (Carl Zeiss, Inc., Thornwood, NY) equipped with a Plan-Apochromat 20×/0.8 numerical aperture objective. Image analysis was performed using Auto-PHLIP-ML, ImageJ, and MATLAB. Biovolumes were determined for the live cells, dead cells, and EPS (con A-stained) components of the biofilm. Total biovolume and thickness were calculated by summing live cells, dead cells, and EPS. Quantitative analysis of the biofilm was also performed by measuring the total protein and organic carbon (TOC) extracted from the membrane surface. Complete biofilm characterization procedures are detailed in the SI.

RESULTS AND DISCUSSION

Chemical Oxidation of Graphite to Graphene Oxide. GO was produced by chemical oxidation of graphite by $KMnO_4$ in concentrated sulfuric and phosphoric acid.[33] These oxidative conditions generated multiple defect sites in the graphitic structure, as indicated by the higher D band intensity in the Raman spectrum of GO (Figure 1a). In carbon nanomaterials, the G band originates from the sp^2-bonded carbon structure while the D band reflects the disorder in the sp^2 structure caused by the presence of defects and sheet edges.[24,38] Compared to graphite, the G/D ratio is decreased from 4.5 to 1.09 after oxidation, indicating a high defect density in GO. The nature of those defects was identified by FTIR and XPS spectroscopy. The FTIR spectrum shows characteristic peaks for sp^2 C=C bonds (1615 cm^{-1}) as well as oxygenated C–O (1220 cm^{-1}), C=O (1720 cm^{-1}), and O–H (3400-3600 cm^{-1}) groups (Figure 1b). Analysis of the XPS C1s spectra reveals that the main oxygenated functional groups are C–O (52%), C=O (7.1%) and O–C=O (5%) (Figure 1c).

The presence of oxygen functional groups in the graphitic structure increases the interlamellar spacing in graphite and allows water to seep in between the graphene layers, facilitating their exfoliation by ultrasonication.[24,26] AFM topographical analysis showed that the exfoliated sheets were ~1.4 nm in thickness (Figure 1 d, e), which is equivalent to single layer GO sheets.[39] The average sheet dimension, determined by SEM imaging, was found to be 0.19 μm^2. A representative SEM image of GO sheets deposited on a silicon wafer is presented in Figure S1.

Graphene Oxide Sheets Possess Strong Antimicrobial Properties. The antimicrobial properties of GO were demonstrated for a wide variety of microorganisms.[26,29–31,40] Cell inactivation has been proposed to be mediated by physical and oxidative interactions leading to a disruption of the membrane integrity and to cell death.[26,29,32,41,42] However, the antimicrobial potential can differ significantly between different GO materials, with some studies indicating high bacterial inactivation while others report no observable toxicity.[29,32,43] This discrepancy can be due to the heterogeneous nature of GO materials generated by different oxidation procedures.[44]

Considering this variable nature of GO, the antimicrobial potential of the GO material produced by our chemical oxidation procedure was verified. When *P. aeruginosa* cells are exposed to a pure GO layer formed by vacuum filtration on a polycarbonate membrane, a decrease in cell viability is observed (Figure S2 a, b). After 1 h of exposure, cell viability decreases from 82% on the control polycarbonate filter to 20% on GO (Figure S2c). Previous studies on the antimicrobial activity of GO deposited on a surface report bacterial inactivation ranging from 59 to 89 % for exposure time of 1-3 h with *E. coli*.[29,45,46] Therefore, the GO produced in this study possesses high antimicrobial activity.

Graphene Oxide Functionalization Changes Surface Properties without Altering Transport Properties. GO sheets were grafted to the polyamide layer through a covalent amide bond formation using ethylenediamine as a cross-linker, as previously described.[32] Successful binding of GO was indicated by SEM imaging. Compared to the pristine membrane (Figure 2a), GO can be visualized as a sheet-like material covering the active layer of the membrane (Figure 2b). This material was confirmed to be GO by Raman spectroscopy, using the I_{1147}/I_{1585} ratio.[32] In TFC membranes, the two dominant Raman peaks originate from the symmetric C−O−C

stretching and phenyl ring vibration of polysulfone, at 1147 and 1585 cm^{-1} (Figure 2c).[47,48] GO, when bound to the membrane, contributes to the Raman signal at 1585 cm^{-1} due to its G band, while its Raman signal at 1147 cm^{-1} is minimal (Figure 1a). After functionalization with GO, the I_{1147}/I_{1585} decreases from 1.47 ± 0.02 for Ctrl membranes to 1.22 ± 0.09 for GO-TFC membranes (Student *t*-test, $p<0.05$), confirming the attachment of GO (Figure 2c). Considering the surface chemistry and covalent binding reaction used for GO surface modification, the amount of GO covering the membrane is hypothesized to be mostly a monolayer of GO, with some overlapping between neighboring GO sheets.

When Ctrl and GO-TFC membranes are characterized using the four-step FO characterization protocol established by Tiraferri *et al.*,[34] no significant impact of GO functionalization is observed on the transport properties of the membrane (Figure S3). These results are in agreement with previous findings showing that the addition of multiple GO layers on TFC membranes did not reduce the water permeability of the membrane.[28] However, the presence of GO on the active layer changes the surface properties of the membrane. After functionalization with GO, the water contact angle of the membrane decreases from 35 ± 4° to 25 ± 3°, indicating that the surface is rendered more hydrophilic (Figure 3a). This change in hydrophilicity cannot be attributed to a change in surface roughness since AFM analysis of pristine and GO-TFC membranes reveals no change in the surface roughness after GO functionalization (Figure S4). Both membranes have an average surface roughness (r_{ms}) of ~ 70 nm (Figure 3b). Therefore, the increased surface hydrophilicity can be attributed to the high density of oxygen functional groups in GO.[24]

Graphene Oxide Imparts Anti-adhesive and Antimicrobial Surface Properties. By increasing surface hydrophilicity, foulant adhesion can be decreased.[10,20] This anti-adhesive effect is due to the formation of a hydration layer opposing the adsorption of biomolecules to the surface.[49] Given this role of hydrophilicity in fouling, increasing the hydrophilicity of the membranes is often used as a strategy to improve their fouling resistance.[10–12,50]

The anti-adhesive properties of GO-TFC were verified by chemical force microscopy using a carboxylated latex particle attached to a tipless AFM cantilever (Figure S5).[35] The high density of carboxyl groups on the particle allows this colloidal probe to be used as a model for fouling since carboxylic groups play an important role in the calcium-mediated foulant

complexation to membranes.[51,52] Chemical force spectroscopy reveals that GO imparts anti-adhesive properties to the surface. Compared to a Ctrl membrane, where the average adhesion force between the colloidal probe and the membrane is -0.49 mN m^{-1} (Figure 4a), GO-TFC membranes have an average adhesion force of -0.15 mN m^{-1} (Figure 4b). The adhesion force distribution on GO-TFC is also characterized with a higher frequency of "NO" events, where the interaction between the probe and the membrane is repulsive and no adhesion is measured. In GO-TFC membranes, 55% of the measurements showed no adhesion, compared to 27% for Ctrl membranes (Figure 4a, b).

Reduced protein adsorption was previously shown for different types of GO-blended polymeric membranes.[27,53,54] Similarly, surface-functionalized RO TFC membranes, where GO was assembled on the surface via a layer-by-layer approach, also showed a reduced adsorption of proteins.[28] Lower fouling propensity of GO-functionalized surfaces can be attributed to an increase in surface hydrophilicity and a smoothing of the membrane surface.[28] However, for GO-TFC, no change in surface roughness is observed after functionalization with GO, suggesting that surface hydrophilicity was the main reason for its anti-adhesive properties. Increased hydrophilicity was also proposed as the mechanism for the lower fouling propensity of poly(vinylidene fluoride) and polyethersulfone membranes mixed with GO.[53,54]

The anti-adhesive properties of GO-TFC membranes were further confirmed by evaluating bacterial adhesion to the membrane. After a 1-h contact time of a *P. aeruginosa* suspension to Ctrl or GO-TFC membranes, cells attached to the membrane were stained with SYTO 9 and PI, enabling cell enumeration and viability assessment (Figure 4c). A lower amount of bacteria is found attached to GO-TFC compared to Ctrl membranes. The number of bacterial cells decreases from 50×10^6 cells per cm^2 to 32×10^6 cells per cm^2 for Ctrl and GO-TFC membranes, respectively (Figure 4d). At the same time, cell viability of bacteria on the surface is also affected, decreasing from 92% for cells attached to the Ctrl membrane to 62% for GO-TFC membrane (Figure 4d). Therefore, GO sheets are still active when bound to the membrane and impart antimicrobial properties as well as anti-adhesive properties to the membrane.

Graphene Oxide Mitigates Biofouling in Forward Osmosis. The anti-adhesive and antimicrobial properties imparted by GO suggest promising biofouling resistance in GO-TFC membranes. However, it should be noted that short-term static assays are not always indicative

of biofouling resistance in membranes. For ultrafiltration and nanofiltration membranes modified with polydopamine or polydopamine-*g*-poly(ethylene glycol), biofouling was not affected despite both reduced protein adsorption and *P. aeruginosa* bacterial adhesion in short term static assays.[17] A similar outcome was obtained with TFC RO membranes modified with anti-adhesive polymer brushes.[16]

In order to accurately determine the biofouling mitigation potential of GO-TFC membranes, dynamic biofouling assays were conducted in a lab-scale cross-flow FO unit. An artificial secondary wastewater medium was used as a feed solution and *P. aeruginosa* were added at an initial concentration of ~6.0×10^7 CFU L^{-1}. Over the course of 24 h, a gradual decline was observed in the permeate flux due to the formation of a biofilm on the membrane. For Ctrl membranes, the flux decline due to biofouling reaches 40% of the initial flux after 24 h of operation, while flux decline for the GO-TFC membranes was 20% (Figure 5a). GO functionalization was thus able to reduce the effect of biofouling on membrane performance.

To understand the role of GO in biofouling mitigation, the membrane was removed from the cell after the 24 h of filtration, and stained for CLSM analysis. Analysis of the side-view of the biofilm reveals important structural differences between the biofilms formed on Ctrl and GO-TFC membranes (Figure 5b). The biofilm layer on GO-TFC is thinner than on Ctrl membranes and a layer of dead cells, shown in red by PI staining, can be observed in the bottom part of the biofilm in contact with the GO-functionalized surface (Figure 5b). This layer of dead cells cannot be observed on the Ctrl membrane, indicating that the antimicrobial activity provided by GO is inactivating bacterial cells in contact with the functionalized surface.

Analysis of the CLSM images was used to quantify the biovolumes of live cells, dead cells, and EPS in the biofilm. These results show that biofilm formed after 24 hours on GO-TFC membranes is thinner and composed of fewer live cells, more dead cells, and smaller EPS biovolumes than biofilms formed on Ctrl membranes (Table 1). Quantitative analysis of the biomass accumulated on the membrane confirms these findings; GO-TFC membranes have less total protein and TOC, both related to bacterial biomass per membrane area than Ctrl membranes (Table 1). Altogether, these results indicate a sparser biofilm development on GO-TFC membranes, an observation that is in agreement with CLSM images (Figure 5c, d). Reduced

accumulation and growth of biomass on the membrane is likely contributed to the lower flux decline observed for GO-TFC membranes under dynamic biofouling conditions.

Implications for Graphene Oxide-Based Biofilm Control. Although numerous studies reported anti-adhesive or antimicrobial membranes using GO,[27,30,32,53–55] very few up to now addressed the more complex issue of biofouling. Biofilm mitigation by GO has been demonstrated for model surfaces like indium tin oxide,[56] or in ultrafiltration membranes used for membrane bioreactors.[57] However, for ultrafiltration membranes, biofouling mitigation was entirely attributed to the anti-adhesive properties of GO incorporated in the polysulfone matrix.[57] In our study, our results show that bacterial inactivation induced by GO sheets also contribute to the reduced biofilm formation on GO-functionalized TFC membranes. These findings provide useful insights into the design of GO-based surfaces for biofouling control, where both anti-adhesive and antimicrobial properties must be considered. The simplicity of membrane functionalization with GO, the absence of detrimental effects on the membrane transport properties, and the possibility of improving both the antimicrobial activity and the hydrophilicity of the membrane selective layer, through changes in sheet size,[46] oxidation level,[29] and nanoscale topography,[58] render GO a viable and attractive material for anti-biofouling membrane development. Future investigations should focus on fine-tuning the physicochemical characteristics of GO to improve both these functionalities. Long-term studies are also needed to assess the stability of the antimicrobial and antifouling properties of GO when exposed to complex water chemistries.

ACKNOWLEDGEMENT

F.P. acknowledges the financial support from the Natural Sciences and Engineering Research Council of Canada. H.J. acknowledges the support of the US National Science Foundation Graduate Research Fellowship (2013162783). Facilities used were supported by the Yale Institute of Nanoscale and Quantum Engineering and NSF MRSEC DMR 1119826. We also thank Prof. Kanani Lee for granting access to the Raman spectrometer.

SUPPORTING INFORMATION

Additional Material and Methods; SEM micrograph of GO sheets deposited on a silicon wafer (Figure S1); Antimicrobial activity of the produced GO sheets (Figure S2); Membrane transport properties of Ctrl and GO-functionalized TFC membranes (Figure S3);AFM 3-D topographical image of Ctrl and GO-TFC membranes (Figure S4); SEM micrograph of the carboxylated-particle attached on a tipless silicon nitride cantilever. (Figure S5); Zeta potential of Ctrl and GO-TFC membranes (Figure S6); Synthetic wastewater composition (Table S1). This material is available free of charge via the Internet at http://pubs.acs.org.

REFERENCES

(1) Shannon, M. A.; Bohn, P. W.; Elimelech, M.; Georgiadis, J. G.; Mariñas, B. J.; Mayes, A. M.; Marinas, B. J.; Mayes, A. M.; Mariñas, B. J.; Mayes, A. M. Science and technology for water purification in the coming decades. *Nature* **2008**, *452*, 301–310.

(2) Wintgens, T.; Melin, T.; Schäfer, A.; Khan, S.; Muston, M.; Bixio, D.; Thoeye, C. The role of membrane processes in municipal wastewater reclamation and reuse. *Desalination* **2005**, *178*, 1–11.

(3) Elimelech, M.; Phillip, W. A. The future of seawater desalination: energy, technology, and the environment. *Science* **2011**, *333* (6043), 712–717.

(4) Shaffer, D. L.; Werber, J. R.; Jaramillo, H.; Lin, S.; Elimelech, M. Forward osmosis : Where are we now ? *Desalination* **2015**, *356*, 271–284.

(5) Mi, B.; Elimelech, M. Organic fouling of forward osmosis membranes: Fouling reversibility and cleaning without chemical reagents. *J. Memb. Sci.* **2010**, *348*, 337–345.

(6) Lee, S.; Boo, C.; Elimelech, M.; Hong, S. Comparison of fouling behavior in forward osmosis (FO) and reverse osmosis (RO). *J. Memb. Sci.* **2010**, *365*, 34–39.

(7) Lutchmiah, K.; Verliefde, R. D.; Roest, K.; Rietveld, L. C.; Cornelissen, E. R. Forward osmosis for application in wastewater treatment: a review. *Water Res.* **2014**, *58*, 179–197.

(8) Achilli, A.; Cath, T. Y.; Marchand, E. A.; Childress, A. E. The forward osmosis membrane bioreactor: A low fouling alternative to MBR processes. *Desalination* **2009**, *238*, 10–21.

(9) Mo, Y.; Tiraferri, A.; Yip, N. Y.; Adout, A.; Huang, X.; Elimelech, M. Improved antifouling properties of polyamide nanofiltration membranes by reducing the density of surface carboxyl groups. *Environ. Sci. Technol.* **2012**, *46*, 13253–13261.

(10) Rana, D.; Matsuura, T. Surface modifications for antifouling membranes. *Chem. Rev.* **2010**, *110*, 2448–2471.

(11) Romero-Vargas Castrillón, S.; Lu, X.; Shaffer, D. L.; Elimelech, M. Amine enrichment and poly(ethylene glycol) (PEG) surface modification of thin-film composite forward osmosis membranes for organic fouling control. *J. Memb. Sci.* **2014**, *450*, 331–339.

(12) Tiraferri, A.; Kang, Y.; Giannelis, E. P.; Elimelech, M. Superhydrophilic thin-film composite forward osmosis membranes for organic fouling control: Fouling behavior and antifouling mechanisms. *Environ. Sci. Technol.* **2012**, *46*, 11135–11144.

(13) Yu, H. Y.; Kang, Y.; Liu, Y.; Mi, B. Grafting polyzwitterions onto polyamide by click chemistry and nucleophilic substitution on nitrogen: A novel approach to enhance membrane fouling resistance. *J. Memb. Sci.* **2014**, *449*, 50–57.

(14) Valladares Linares, R.; Yangali-Quintanilla, V.; Li, Z.; Amy, G. NOM and TEP fouling of a forward osmosis (FO) membrane: Foulant identification and cleaning. *J. Memb. Sci.* **2012**, *421-422*, 217–224.

(15) Flemming, H. C.; Schaule, G.; Griebe, T.; Schmitt, J.; Tamachkiarowa, a. Biofouling - the Achilles heel of membrane processes. *Desalination* **1997**, *113*, 215–225.

(16) Bernstein, R.; Freger, V.; Lee, J.-H.; Kim, Y.-G.; Lee, J.; Herzberg, M. "Should I stay or should I go?" Bacterial attachment vs biofilm formation on surface-modified membranes. *Biofouling* **2014**, *30*, 367–376.

(17) Miller, D. J.; Araújo, P. A.; Correia, P. B.; Ramsey, M. M.; Kruithof, J. C.; van Loosdrecht, M. C. M.; Freeman, B. D.; Paul, D. R.; Whiteley, M.; Vrouwenvelder, J. S. Short-term adhesion and long-term biofouling testing of polydopamine and poly(ethylene glycol) surface modifications of membranes and feed spacers for biofouling control. *Water Res.* **2012**, *46*, 3737–3753.

(18) Blok, A. J.; Chhasatia, R.; Dilag, J.; Ellis, A. V. Surface initiated polydopamine grafted poly([2-(methacryoyloxy)ethyl]trimethylammonium chloride) coatings to produce reverse osmosis desalination membranes with anti-biofouling properties. *J. Memb. Sci.* **2014**, *468*, 216–223.

(19) Ben-Sasson, M.; Lu, X.; Bar-Zeev, E.; Zodrow, K. R.; Nejati, S.; Qi, G.; Giannelis, E. P.; Elimelech, M. In situ formation of silver nanoparticles on thin-film composite reverse osmosis membranes for biofouling mitigation. *Water Res.* **2014**, *62*, 260–270.

(20) Kochkodan, V.; Hilal, N. A comprehensive review on surface modified polymer membranes for biofouling mitigation. *Desalination* **2015**, *356*, 187–207.

(21) Rahaman, M. S.; Thérien-Aubin, H.; Ben-Sasson, M.; Ober, C. K.; Nielsen, M.; Elimelech, M. Control of biofouling on reverse osmosis polyamide membranes modified with biocidal nanoparticles and antifouling polymer brushes. *J. Mater. Chem. B* **2014**, *2*, 1724.

(22) Zhang, S.; Qiu, G.; Ting, Y. P.; Chung, T. S. Silver-PEGylated dendrimer nanocomposite coating for anti-fouling thin film composite membranes for water treatment. *Colloids Surfaces A Physicochem. Eng. Asp.* **2013**, *436*, 207–214.

(23) Ye, G.; Lee, J.; Perreault, F.; Elimelech, M. Controlled Architecture of Dual-functional Block Copolymer Brushes on Thin-Film Composite Membranes for Integrated "Defending" and "Attacking" Strategies against Biofouling. *ACS Appl. Mater. Interfaces* **2015**, *7*, 23069–23079.

(24) Dreyer, D. R.; Park, S.; Bielawski, C. W.; Ruoff, R. S. The chemistry of graphene oxide. *Chem. Soc. Rev.* **2010**, *39*, 228–240.

(25) Hegab, H. M.; Zou, L. Graphene oxide-assisted Membranes: Fabrication and potential Applications in desalination and water purification. *J. Memb. Sci.* **2015**, *484*, 95–106.

(26) Perreault, F.; Faria, A. F. De; Elimelech, M.; Fonseca de Faria, A.; Elimelech, M.; Faria, A. F. De; Elimelech, M. Environmental applications of graphene-based nanomaterials. *Chem. Soc. Rev.* **2015**, *44*, 5861–5896.

(27) Zinadini, S.; Zinatizadeh, A. A.; Rahimi, M.; Vatanpour, V.; Zangeneh, H. Preparation of a novel antifouling mixed matrix PES membrane by embedding graphene oxide nanoplates. *J. Memb. Sci.* **2014**, *453*, 292–301.

(28) Choi, W.; Choi, J.; Bang, J.; Lee, J.-H. Layer-by-layer assembly of graphene oxide nanosheets on polyamide membranes for durable reverse-osmosis applications. *ACS Appl. Mater. Interfaces* **2013**, *5*, 12510–12519.

(29) Akhavan, O.; Ghaderi, E. Toxicity of graphene and graphene oxide nanowalls against bacteria. *ACS Nano* **2010**, *4*, 5731–5736.

(30) Musico, Y. L. F.; Santos, C. M.; Dalida, M. L. P.; Rodrigues, D. F. Surface Modification of Membrane Filters Using Graphene and Graphene Oxide-Based Nanomaterials for Bacterial Inactivation and Removal. *ACS Sustain. Chem. Eng.* **2014**, *2*, 1559–1565.

(31) Sanchez, V. C.; Jachak, A.; Hurt, R. H.; Kane, A. B. Biological interactions of graphene-family nanomaterials: an interdisciplinary review. *Chem. Res. Toxicol.* **2012**, *25*, 15–34.

(32) Perreault, F.; Tousley, M. E.; Elimelech, M. Thin-Film Composite Polyamide Membranes Functionalized with Biocidal Graphene Oxide Nanosheets. *Environ. Sci. Technol. Lett.* **2014**, No. 1, 71–76.

(33) Marcano, D. C.; Kosynkin, D. V; Berlin, J. M.; Sinitskii, A.; Sun, Z.; Slesarev, A.; Alemany, L. B.; Lu, W.; Tour, J. M. Improved synthesis of graphene oxide. *ACS Nano* **2010**, *4*, 4806–4814.

(34) Tiraferri, A.; Yip, N. Y.; Straub, A. P.; Romero-Vargas Castrillon, S.; Elimelech, M. A method for the simultaneous determination of transport and structural parameters of forward osmosis membranes. *J. Memb. Sci.* **2013**, *444*, 523–538.

(35) Li, Q.; Elimelech, M. Organic Fouling and Chemical Cleaning of Nanofiltration Membranes: Measurements and Mechanisms. *Environ. Sci. Technol.* **2004**, *38*, 4683–4693.

(36) Glueckstern, P.; Priel, M.; Gelman, E.; Perlov, N. Wastewater desalination in Israel. *Desalination* **2008**, *222*, 151–164.

(37) Bar-Zeev, E.; Zodrow, K. R.; Kwan, S. E.; Elimelech, M. The importance of microscopic characterization of membrane biofilms in an unconfined environment. *Desalination* **2014**, *348*, 8–15.

(38) Tuinstra, F.; Koenig, L. Raman Spectrum of Graphite. *J. Chem. Phys.* **1970**, *53*, 1126–1130.

(39) Mcallister, M. J.; Li, J.; Adamson, D. H.; Schniepp, H. C.; Abdala, A. A.; Liu, J.; Herrera-alonso, M.; Milius, D. L.; Car, R.; Prud'homme, R. K.; et al. Single Sheet Functionalized Graphene by Oxidation and Thermal Expansion of Graphite. *Chem. Mater.* **2007**, *19*, 4396–4404.

(40) Chen, J.; Peng, H.; Wang, X.; Shao, F.; Yuan, Z.; Han, H. Graphene oxide exhibits broad-spectrum antimicrobial activity against bacterial phytopathogens and fungal conidia by intertwining and membrane perturbation. *Nanoscale* **2014**, *6*, 1879–1889.

(41) Castrillón, S. R.-V.; Perreault, F.; de Faria, A. F.; Elimelech, M. Interaction of Graphene Oxide with Bacterial Cell Membranes: Insights from Force Spectroscopy. *Environ. Sci. Technol. Lett.* **2015**, *2*, 112–117.

(42) Li, Y.; Yuan, H.; von dem Bussche, A.; Creighton, M.; Hurt, R. H.; Kane, A. B.; Gao, H. Graphene microsheets enter cells through spontaneous membrane penetration at edge asperities and corner sites. *Proc. Natl. Acad. Sci. U. S. A.* **2013**, *110*, 12295–12300.

(43) Ruiz, O. N.; Fernando, K. A S.; Wang, B.; Brown, N. A; Luo, P. G.; McNamara, N. D.; Vangsness, M.; Sun, Y.-P.; Bunker, C. E. Graphene oxide: a nonspecific enhancer of cellular growth. *ACS Nano* **2011**, *5*, 8100–8107.

(44) Dreyer, D. R.; Todd, A. D.; Bielawski, C. W. Harnessing the chemistry of graphene oxide. *Chem. Soc. Rev.* **2014**, *43*, 5288.

(45) Mangadlao, J. D.; Santos, C. M.; Felipe, M. J. L.; Leon, A. C. C. De; Rodrigues, D. F. On the antibacterial mechanism of graphene oxide (GO) Langmuir – Blodgett films. *Chem. Commun.* **2015**, *1*, 1–4.

(46) Perreault, F.; de Faria, A. F.; Nejati, S.; Elimelech, M. Antimicrobial Properties of Graphene Oxide Nanosheets : Why Size Matters. *ACS Nano* **2015**, *9*, 7226–7236.

(47) Shilton, S. J.; Prokhorov, K. A; Gordeyev, S. A; Nikolaeva, G. Y.; Dunkin, I. R.; Smith, W. E.; Pashinin, P. P. Raman spectroscopic evaluation of molecular orientation in polysulfone. *Laser Phys. Lett.* **2004**, *1*, 336–339.

(48) Kim, H. J.; Fouda, A. E.; Jonasson, K. In Situ Study on Kinetic Behavior during Asymmetric Membrane Formation via Phase Inversion Process Using Raman Spectroscopy. *J. Appl. Polym. Sci.* **1999**, *75*, 135–141.

(49) Morra, M. On the molecular basis of fouling resistance. *J. Biomater. Sci. Polym. Ed.* **2000**, *11*, 547–569.

(50) Shaffer, D. L.; Jaramillo, H.; Romero-Vargas Castrillón, S.; Lu, X.; Elimelech, M. Post-fabrication modification of forward osmosis Membranes with a poly(ethylene glycol) block copolymer for improved organic fouling resistance. *J. Memb. Sci.* **2015**, *490*, 209–219.

(51) Ang, W. S.; Elimelech, M. Protein (BSA) fouling of reverse osmosis membranes: Implications for wastewater reclamation. *J. Memb. Sci.* **2007**, *296*, 83–92.

(52) Mo, Y.; Xiao, K.; Shen, Y.; Huang, X. A new perspective on the effect of complexation between calcium and alginate on fouling during nanofiltration. *Sep. Purif. Technol.* **2011**, *82*, 121–127.

(53) Jin, F.; Lv, W.; Zhang, C.; Li, Z.; Su, R.; Qi, W.; Yang, Q.-H.; He, Z. High-performance ultrafiltration membranes based on polyethersulfone–graphene oxide composites. *RSC Adv.* **2013**, *3*, 21394.

(54) Zhao, C.; Xu, X.; Chen, J.; Yang, F. Optimization of preparation conditions of poly(vinylidene fluoride)/graphene oxide microfiltration membranes by the Taguchi experimental design. *Desalination* **2014**, *334*, 17–22.

(55) Soroush, A.; Ma, W.; Silvino, Y.; Rahaman, M. S. Surface modification of thin film composite forward osmosis membrane by silver-decorated graphene-oxide nanosheets. *Environ. Sci. Nano* **2015**, *2*, 395–405.

(56) Mejías Carpio, I. E.; Santos, C. M.; Wei, X.; Rodrigues, D. F. Toxicity of a polymer-graphene oxide composite against bacterial planktonic cells, biofilms, and mammalian cells. *Nanoscale* **2012**, *4*, 4746–4756.

(57) Lee, J. J.; Chae, H.-R.; Won, Y. J.; Lee, K.; Lee, C.-H.; Lee, H. H.; Kim, I.-C.; Lee, J. J. Graphene oxide nanoplatelets composite membrane with hydrophilic and antifouling properties for wastewater treatment. *J. Memb. Sci.* **2013**, *448*, 223–230.

(58) Rafiee, J.; Rafiee, M. A.; Yu, Z. Z.; Koratkar, N. Superhydrophobic to superhydrophilic wetting control in graphene films. *Adv. Mater.* **2010**, *22*, 2151–2154.

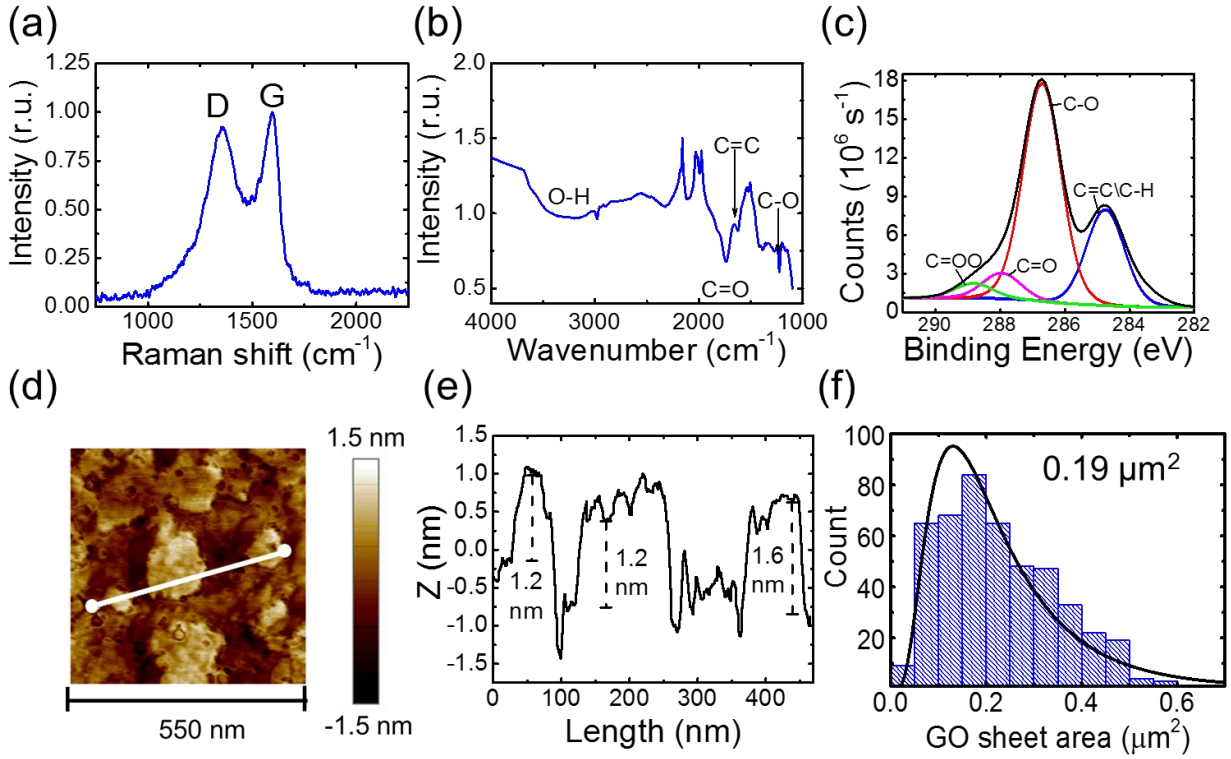

FIGURE 1. Characterization of GO nanosheets. (a) Raman spectroscopy of GO, indicating the characteristic G and D bands of carbon nanomaterials; (b) FTIR spectrum identifying the different functional groups of GO; (c) C1s XPS spectrum of GO, identifying the relative abundance of the different functional groups; (d) representative AFM image of GO sheets. The white bar indicates the thickness profile represented in (e); (e) representative sheet thickness profile obtained by AFM, indicating that GO sheets were mostly single-layer GO. (f) GO sheet area distribution, determined by image analysis of at least 2000 individual sheets obtained by SEM.

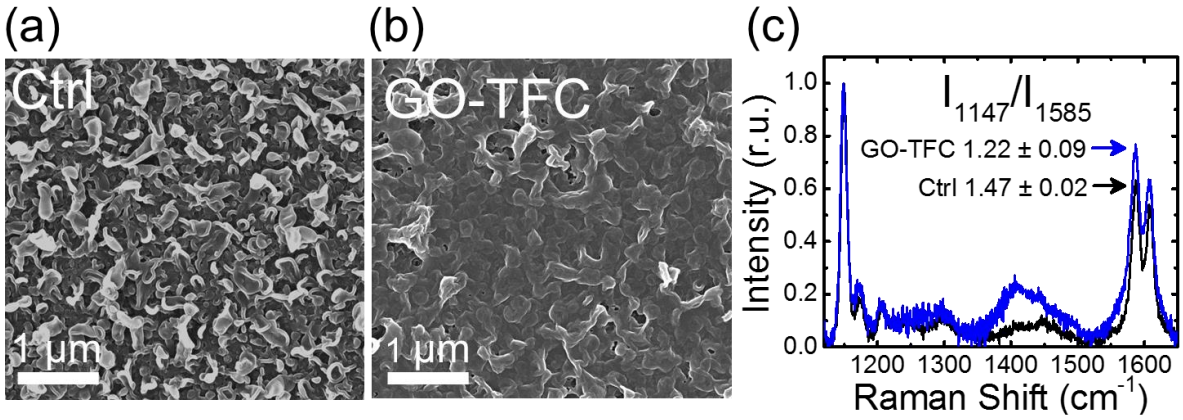

FIGURE 2. Characterization of TFC membranes. (a, b) Representative SEM micrographs of the polyamide active layer before (a) and after (b) functionalization with GO. (c) Raman spectroscopy of Ctrl and GO-functionalized TFC membranes. The ratio between the peaks at 1147 and 1585 cm^{-1} is used as an indicator of the presence of GO on the membrane.

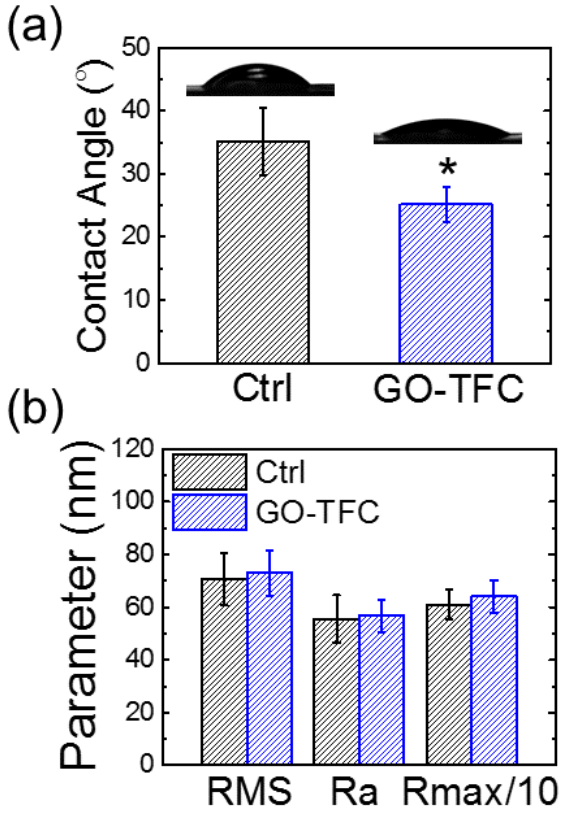

FIGURE 3. Membrane properties of pristine and GO-TFC membranes. (a) Water contact angle of Ctrl and GO-functionalized membranes. (b) Surface roughness of Ctrl and GO-functionalized membranes. RMS is the root mean-square of roughness, R_a is the average roughness, and R_{max} is the maximum roughness. Star indicates statistical significance, determined by a student's *t*-test (p-value < 0.05).

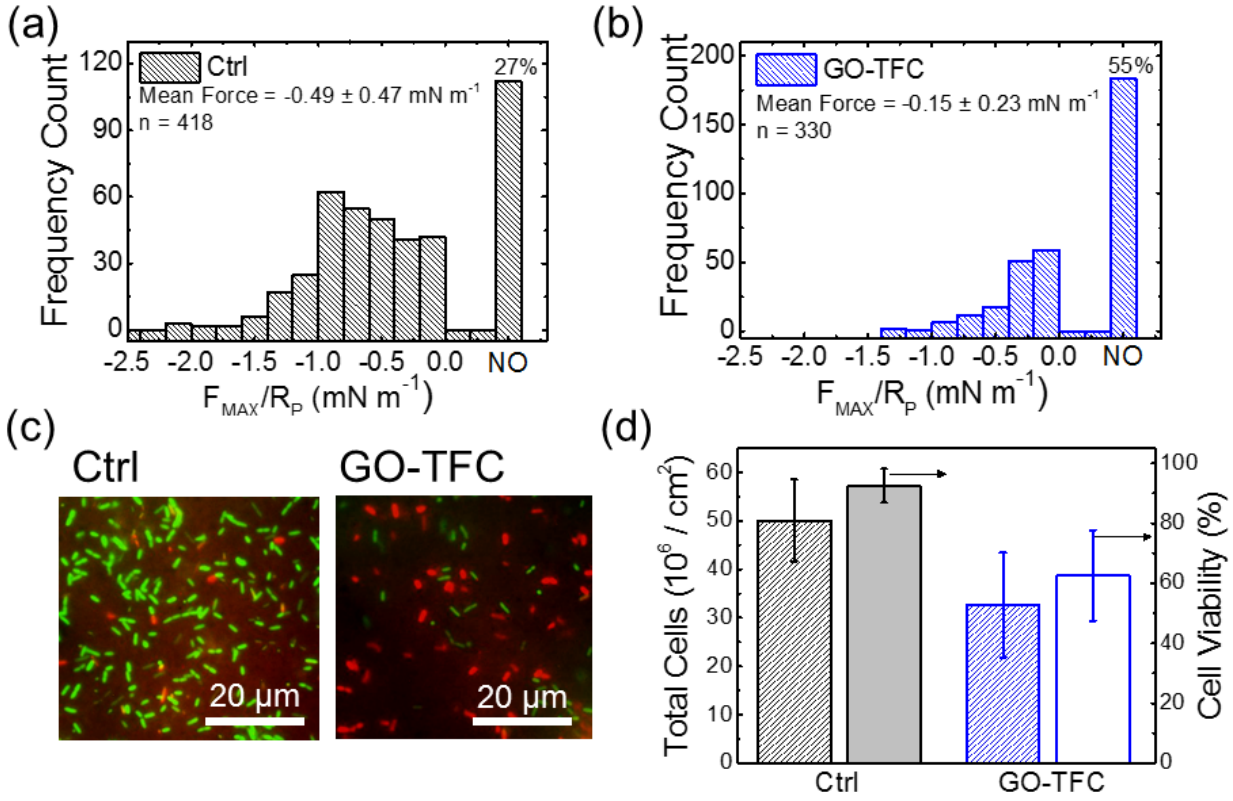

FIGURE 4. (a-b) Distribution of adhesion forces between a carboxylated latex particle probe and Ctrl (a) and GO-TFC (b) membranes. For each membrane, at least 300 force measurements, sampled over five randomly selected locations, were obtained. The columns labeled "NO" indicate measurements where the probe–membrane interactions were too weak to be differentiated from random fluctuations, and are considered as no adhesion. (c) Representative epifluorescence microscopy images of *P. aeruginosa* cells on Ctrl and GO-TFC membranes. Bacterial cells were stained with SYTO 9 (green), and PI (red) for "live" and "dead" cells, respectively. (d) Total number of *P. aeruginosa* cell adhered to the surface of Ctrl and GO-TFC membranes, and cell viability of adhered *P. aeruginosa* cells after 1 h of contact. Star indicates statistical significance, determined by a student's *t*-test (p-value < 0.05).

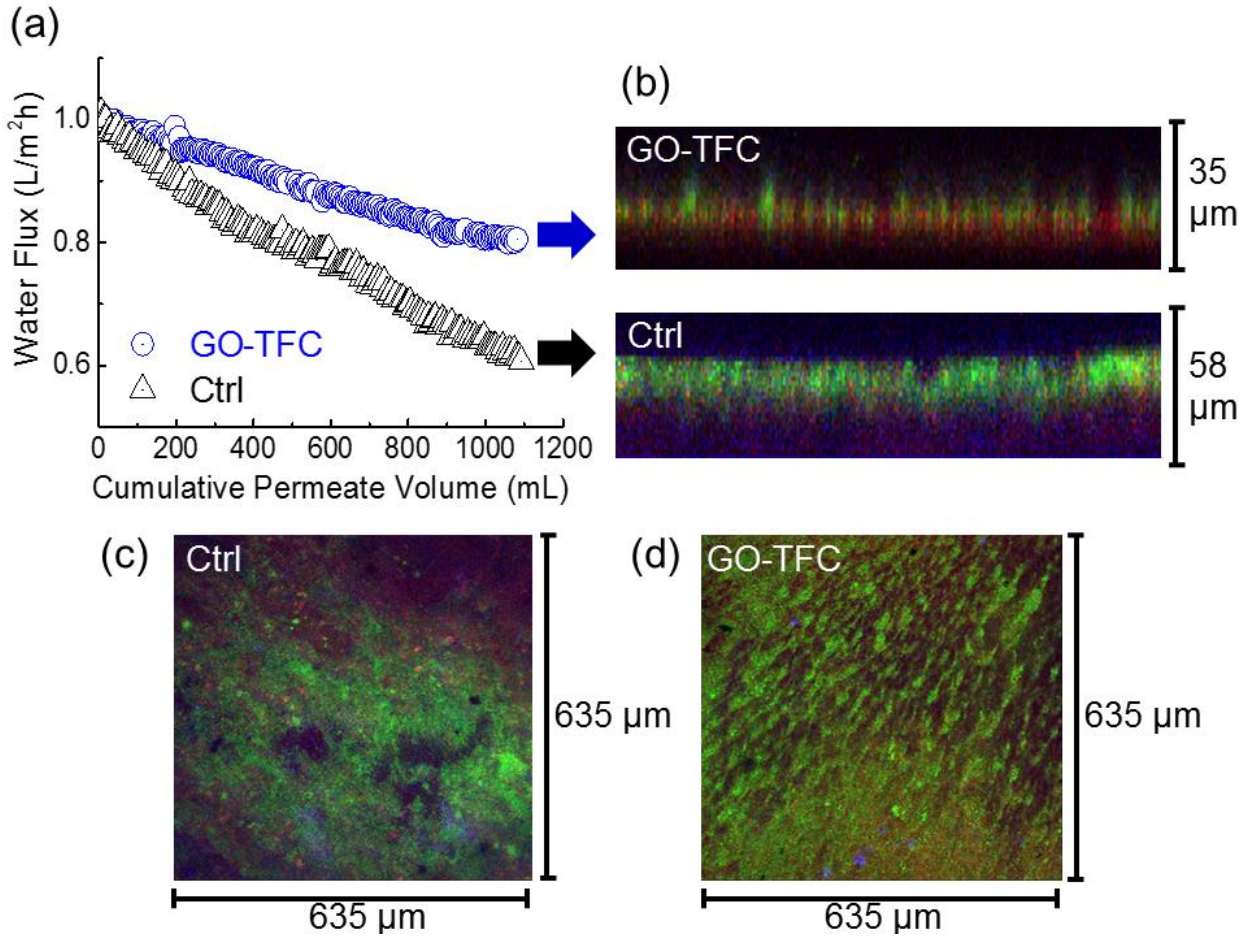

FIGURE 5. (a) Normalized water fluxes of Ctrl and GO-functionalized membrane as a function of cumulative permeate flux in biofouling experiments using *P. aeruginosa*. Feed solution was composed of synthetic wastewater matrix and 1 M NaCl was used as the draw solution. (b) Representative confocal microscopy side view of the biofilms formed on Ctrl and GO-TFC membranes after 24 h of FO operation. (c-d) Representative confocal microscopy top view of the biofilms formed on Ctrl (c) and GO-TFC (d) membranes after 24 h of FO operation. Biofilm coverage of the membrane surface is reduced by functionalization with GO. Biofilms were stained with Con A (blue), SYTO 9 (green), and PI (red) for EPS (polysaccharides), "live", and "dead" cells, respectively.

TABLE 1: Biofilm characteristics of pristine and GO-functionalized membranes

Parameters	biofilm thickness [a] (μm)	"live" cell biovolume [a] ($\mu m^3/\mu m^2$)	"dead" cell biovolume [a] ($\mu m^3/\mu m^2$)	EPS biovolume [a] ($\mu m^3/\mu m^2$)	TOC biomass [b] (pg/um^2)	total protein mass [b] (pg/um^2)
Pristine membrane	58 ± 4	15.1 ± 2.3	10.3 ± 2.1	9.8 ± 1.5	0.47 ± 0.04	49.5 ± 5.1
GO modified membrane	35 ± 6	10.2 ± 3.4	14.5 ± 2.8	7.9 ± 2.4	0.18 ± 0.11	23.9 ± 3.5

[a] biofilm thickness and biovolume were averaged, with standard deviation (SD) calculated from ten random samples in duplication experiments. [b] Average TOC and protein biomasses were presented with SD calculated from four measurements of two membrane coupons.